Australian Meteorological and Oceanographic Journal 63 (2013) 15–26

Simulated and projected summer rainfall in tropical Australia: links to atmospheric circulation using the CSIRO-Mk3.6 climate model

Ramasamy Suppiah[1], Mark Collier[1], Stephen Jeffrey[2], Leon Rotstayn[1], Jozef Syktus[2] and Kenneth Wong[2].

[1]Centre for Australian Weather and Climate Research,
CSIRO Marine and Atmospheric Research, Aspendale, Australia
[2]Queensland Department of Science, Information Technology, Innovation and the Arts,
Dutton Park, Australia

(Manuscript received July 2012; revised April 2013)

Simulations of mean climate characteristics and atmospheric circulation patterns in the tropical region of Australia during the austral summer (December to February) are assessed by comparing against observations. An examination of the observed climatologies of mean sea level pressure, winds at lower and upper levels and rainfall with simulated climatologies show that the model captures the spatial structures of observed patterns fairly well. However, there are some discrepancies in the magnitudes between observed and modelled parameters. The model can reasonably reproduce the observed link between tropical Australian rainfall variability and the atmospheric circulation patterns. Changes in circulation patterns and rainfall are investigated for Representative Concentration Pathways (RCPs) 4.5 and 8.5. Spatial patterns of changes in circulation parameters and rainfall are very similar for both RCP 4.5 and RCP 8.5, but the magnitudes are larger for the RCP 8.5. Under anthropogenic climate change conditions, the CSIRO-Mk3.6 climate model simulates an atmospheric circulation pattern reflecting weaker monsoon conditions in the Australian region, and hence, reduced rainfall over tropical Australia. A slightly increased pressure over northwest Australia and slightly decreased pressure over north Asia is simulated. Winds at lower and upper tropospheric levels indicate opposing anomalies and reduced rainfall over a broader region that encompasses northern Australia, parts of Indonesia and around the Philippines. However, an increase in rainfall is simulated for the region east of Papua New Guinea.

Introduction

Tropical Australia, which covers the northern parts of Western Australia, Northern Territory and Queensland, has a rich diversity of habitats that sustain regional economies such as mining, grazing, fisheries and tourism. The region experiences a wet–dry monsoon climate that is highly variable on daily to interannual and inter-decadal timescales. The variability is linked to various climate drivers, such as the Madden-Julian Oscillation, the El Niño-Southern Oscillation, Indian Ocean Dipole and the Pacific Decadal Oscillation (Suppiah and Wu 1998, Risbey et al. 2009, Klingamon et al. 2012). In addition, climate change is a potential threat that, in the long term, could affect the spatial distribution of diverse fauna and flora, particularly in Kakadu National Park and the tropical rainforest region (Suppiah et al 2010).

Most global climate models simulate anthropogenic-related increases in temperature but large uncertainties are associated with projected changes in rainfall (Suppiah et al. 2007, CSIRO and Bureau of Meteorology 2007, Smith and Chandler 2009). A significant change in mean rainfall and/or changes in heavy rain events could be detrimental to the ecosystem. Ecological modelling suggests that some

Corresponding author address: Ramasamy Suppiah, CSIRO Marine and Atmospheric Research, Private Bag 1, Aspendale, Vic. 3195. Email: suppiah.ramasamy@csiro.au

species may disappear due to increased temperature and reduced rainfall, particularly in the rainforest region of northeast Queensland (Williams et al. 2010). In this study, we analyse the results of the CSIRO Mark 3.6 (CSIRO-Mk3.6) climate model simulations performed for the Coupled Model Intercomparison Project phase 5 (CMIP5) (Taylor et al. 2012). We focus on projected changes to rainfall over tropical Australia using methods similar to those used to assess CMIP3 simulations as described by Suppiah et al. (2007).

Assessment of CMIP3 model simulations showed that most of the models are able to capture the spatial patterns of long-term rainfall climatology in northern Australia; however, most of the CMIP3 models failed to simulate rainfall variability on interannual timescale over monsoon regions (Kim et al. 2008, Suppiah et al. 2012). The limitations associated with simulated rainfall and the subsequent implications for ecological modelling are further complicated by the fact that model projections show large uncertainties towards the end of the 21st century. Like most of the IPCC AR4 models, the CSIRO-Mk3.6 model captures the observed temporal patterns of global surface temperature (Rotstayn et al. 2012). Observations and simulations show an increase in surface temperature from 1851 to 1940, a dip between 1940 and 1960, and stronger increase from 1960 onwards. Models also show large uncertainty in terms of simulated rainfall at the end of 21st century. For further discussion of the merits and demerits of models see Räisänen (2007).

In this paper we focus on projected changes in rainfall over tropical Australia, using the new CMIP5 results and analysis methods similar to those used to assess CMIP3 simulations (as described by Suppiah et al. 2007). Firstly, we provide a brief description of the model, along with the methods used and the modelled and observed datasets. Secondly, simulated long-term climatologies are assessed against observed climatologies of mean sea level pressure, winds at lower and upper levels, and rainfall. Thirdly, the model's capability of simulating the link between tropical Australian rainfall variability and atmospheric circulation patterns is described using a correlation analysis. Finally, we describe projected changes in mean and extreme rainfall and winds over the broad region centred on tropical Australia for RCP 4.5 and 8.5.

CSIRO Mark 3.6 GCM

The CSIRO-Mk3.6 climate model is a coupled atmosphere-ocean model with dynamic sea ice. The atmospheric component has 18 vertical levels and a horizontal resolution of approximately 1.875° × 1.875° (spectral T63). It was developed from the earlier Mark 3.5 version (Gordon et al. 2002, 2010, Smith 2007, Collier et al. 2011a, 2011b). The main differences include the inclusion of an interactive aerosol treatment and an updated radiation scheme (see Rotstayn et al. 2013).

In this study, we analyse the results of the CSIRO-Mk3.6 climate model simulations performed for the Coupled Model Intercomparison Project phase 5 (CMIP5) (Taylor et al. 2012). The CMIP5 experiments used a new range of forcing scenarios characterised by Representative Concentration Pathways (RCPs), rather than the earlier emission scenarios used in CMIP3 which were based on the Special Report on Emissions Scenarios (SRES) (IPCC 2007). SRES scenarios were based on a set of socioeconomic assumptions that lead to estimations of anthropogenic emissions, concentrations and land-cover change projections. The new RCPs are based on a range of assumptions about socioeconomic activities characterised for the purpose of climate modelling as a radiative forcing driving climate system throughout the 21st century. Figure 1 shows a comparison of the projected concentration of carbon dioxide under SRES (A1B, A1FI, A2 and B1) emission scenarios and RCPs (2.6, 4.5, 6.0 and 8.5) approaches. The high and low (A1FI and B1, respectively) SRES scenarios closely follow the CO_2 concentrations of RCPs of 8.5 and 4.5. However, the RCPs do not correspond closely to the SRES scenarios because other aspects of the forcings differ strongly, especially the sources and distribution of anthropogenic aerosols.

Model and observed data

Our study is restricted to the region 45ºS–45ºN, 50ºE–130ºW. A subset of this domain (10–20°S, 110–160°E) covering the tropical region of Australia was selected to compute area-average rainfall. Both smaller and larger regions are shown in Fig. 2. The larger domain was used to assess model simulations against observed climatologies and the link between rainfall and atmospheric circulation patterns. The observed long-term climatology of mean rainfall for December–February is also shown from the Australian Water Availability Project (AWAP; Jones et al. 2009) data.

Model data used in this study were taken from three CMIP5 experiments: (i) an historical simulation from 1850 to 2005 using both natural and anthropogenic forcings (HIST);

Fig. 1. Comparison of CO_2 concentrations from SRES (A1B, A1FI, A2, B1) and RCPs (2.6/3.0-PD, 4.5, 6.0, 8.5) approaches. Source: Meinshausen et al. (2011).

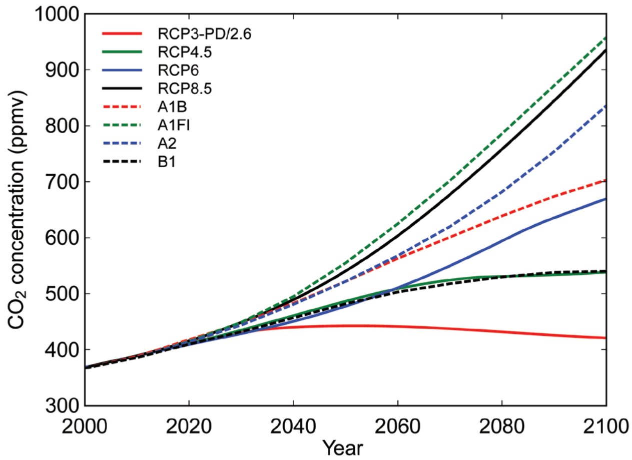

Fig. 2. Domain of interest (45°N–45°S, 50°E–130°W) and the region encompassing tropical Australia (10–20°S, 110–160°E). Long-term rainfall for summer (December to February) is also shown over Australia as mm per day. Source: AWAP.

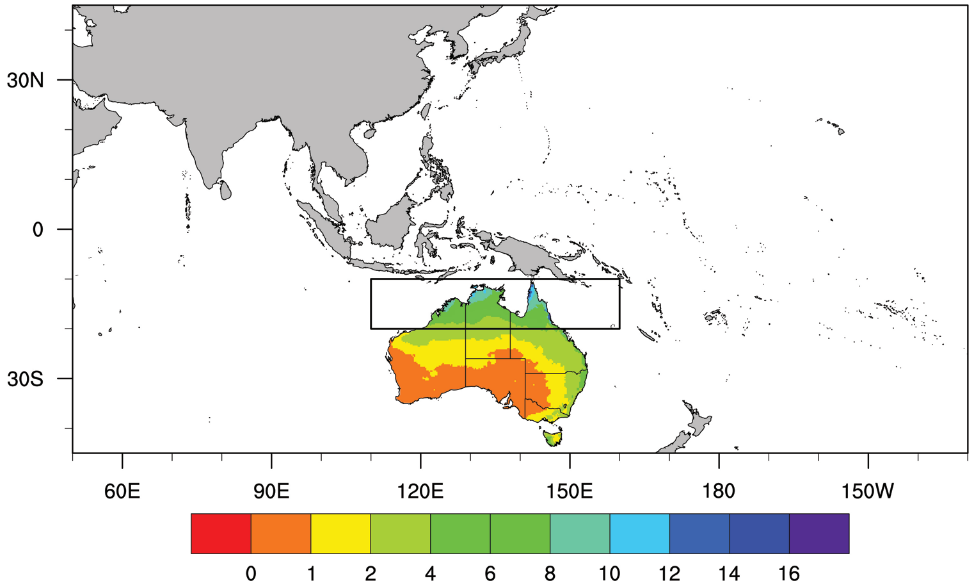

and (ii) projection experiments from 2006 to 2100 using RCPs 4.5 and 8.5 (RCP4.5 and RCP8.5, respectively). The RCP 4.5 and 8.5 simulations were analysed to investigate the range of potential changes and also any changes to circulation patterns in the future. For further details about the CSIRO-Mk3.6 CMIP5 experiments, see Jeffrey et al. (2013). All experiments were run using a ten member ensemble and in this work the ensemble average was used to assess against observations. Land and ocean points are used to calculate simulated area-averaged monthly rainfall over the tropical Australian region and compared with GPCP observed data.

The gridded AWAP daily rainfall dataset from 1979–2005 at 0.25° × 0.25° resolution is derived from quality controlled station data and covers only the land area of the Australian continent. Rainfall data (1979–2005) from the Global Precipitation Climatology Project (GPCP) (Alder et al. 2003) was also used as this dataset covers both ocean and land regions. National Center for Environmental Prediction (NCEP) reanalysis data (Kalnay et al. 1996) for the period 1971–2005 for mean sea level pressure and winds at various levels was also used. The AWAP and GPCP datasets were used for analyses targeting the tropical Australia region, and the NCEP datasets were used for analyses spanning the larger domain that include land and ocean areas.

Methods

The statistical measures used to assess model results include pattern correlation and root mean square (RMS) error values. Long-term climatologies were constructed for mean sea level pressure, and zonal (u) and meridional (v) winds at 850 hPa and 200 hPa over the region 45°S–45°N, 50°E–130°W (see Fig. 2) for both observations (NCEP Reanalysis) and historical simulations (HIST) for the period 1971–2005. The long-term climatology for rainfall was constructed using AWAP data from 1979 to 2005. Although the dataset is available for a longer period, we selected the period 1979–2005 for consistency with the length of the GPCP dataset, also used in this study. The ability of the model to capture the relationship between rainfall variability and atmospheric circulation was assessed using correlations and regression analyses between the area-averaged rainfall and mean sea level pressure and winds at lower and upper levels. The relationship between the tropical Australian monsoon and winds is shown using a vector representation.

Results

Mean summer (DJF) climate simulations

The current generation of GCMs has difficulty in reproducing the spatial and temporal characteristics of observed rainfall. By comparison, model simulations of temperature are generally regarded as being reliable (IPCC 2007). The model to model variations in simulated rainfall are typically large in terms of the spatial and temporal patterns in both historical and future climate simulations. However, the annual cycle of rainfall is fairly well captured by most models, although there are differences in magnitudes when compared with observations. It is also worth mentioning that there are differences in the spatial and temporal characteristics of the various observational datasets which are available. A comparison of the observed AWAP (land only) and CSIRO-Mk3.6 GCM simulated annual cycle of tropical Australian rainfall is shown in Fig. 3. The results indicate the CSIRO-Mk3.6 model reproduces the annual cycle with the wet season from November to April and the dry season from May to October. The model tends to over-estimate the rainfall in the first half of the year (January to June) and underestimate the rainfall in the last half of the year (July to December). Coefficient variations are small during the monsoonal months and relatively large during the dry season (June to August). A comparison between the model simulated annual cycle and the annual cycle from GPCP (Alder et al. 2003), which has both land and ocean points, shows good agreement (not shown). This suggests that the model fairly well captures the annual cycle over the study domain when compared to two observational datasets.

In the remainder of this section we compare the observed and simulated climatologies of selected variables for the austral summer (December–January–February, DJF). Figure 4 compares the DJF climatologies for mean sea-level pressure (MSLP) over the period 1971–2005. The model simulates the basic features of the observed spatial pattern with broad low pressure regions over the western and northern Pacific Ocean, and the high pressure regions over eastern Asia and the southern Indian Ocean. The pattern correlation between observed and simulated mean sea level pressure is 0.95 with an RMS error of 2.0 hPa. Although the model reproduces the dominant high and low pressure regions, there are differences in the magnitudes between observed and simulated pressure values. In particular, the simulated pressures over the northern Pacific Ocean and Indonesian/Australian regions are lower than observed. In contrast the simulated values are slightly higher than the observed values over the mountainous regions of south and southeast Asia. The model captures the climatological values over the Pacific and Indian Ocean regions reasonably well.

Observed and simulated winds in the lower atmosphere (850 hPa) are compared in Fig. 5. The figure indicates that the model captures many of the circulation patterns including north easterlies over southeast Asia, westerlies over the Indonesian/north Australian region, southerlies over the west coast of Western Australia, south easterlies over the Coral Sea and southern half of the Australian continent. The model also captures the anti-cyclonic circulation over the southern Indian Ocean and the wind patterns over the equatorial and northern Pacific Ocean. The difference between observed and simulated winds indicates that the model tends to overestimate the magnitudes of winds over east and southeast Asia and east of Papua New Guinea. In the latter case, the overestimation has been linked to the cold tongue intrusion in the model simulation (Rotstayn et al. 2012). The impact of the cold tongue will also be discussed in relation to rainfall and circulation changes. Apart from these discrepancies, the model simulates the low level wind pattern over the tropical Australian region fairly well. For a detailed discussion of how large-scale circulation patterns western Pacific were reproduced by IPCC CMIP3 models, see Smith et al. (2012).

Observed and simulated DJF upper-level (200 hPa) winds are shown in Fig. 6. The dominant features include an anti-cyclonic circulation over the Indonesian/north Australian region, and strong westerlies south of the Australian continent and over the Himalayas. Winds are easterly over

Fig. 3. Observed and CSIRO-Mk3.6 simulated monthly climatological rainfall for tropical Australia over the period 1979–2005. Coefficient of variations for simulated rainfall are derived from ten ensemble members. Land-only points are used to calculate simulated average rainfall for tropical Australia. Observed values over land points are from the AWAP data set. Units are mm per day.

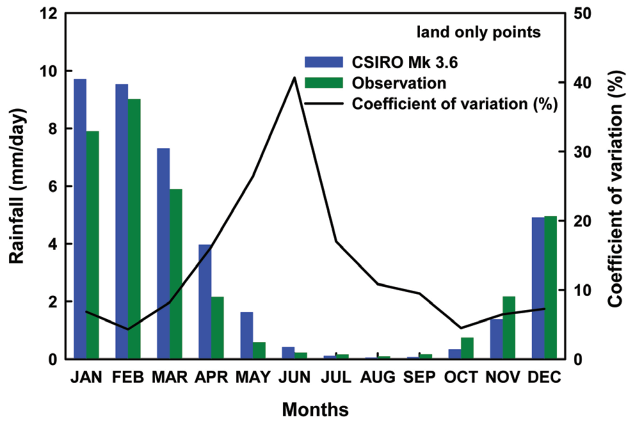

Fig. 4. Observed (a) and simulated (b) climatologies for December–January–February mean sea level pressure for the period 1971–2005; and the difference between observed and simulated pressure patterns (c). Units are hPa. Source for observational data: NCEP reanalysis (Kalnay et al. 1996).

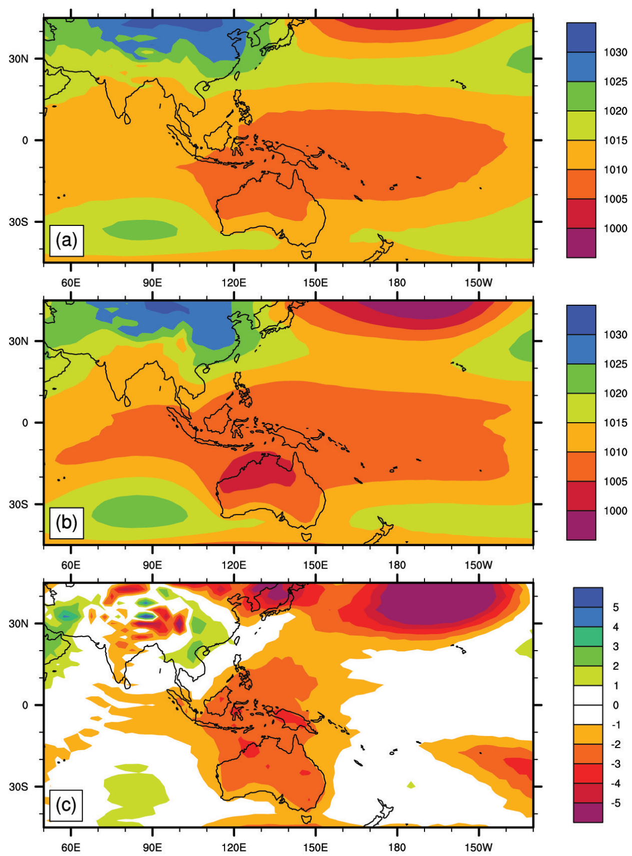

Fig. 5. Observed (a) and simulated (b) climatologies for December–January–February 850 hPa wind for the period 1971–2005; and the difference between observed and simulated pressure patterns (c). Vector scales are in m s^{-1}. Source for observational data: NCEP reanalysis (Kalnay et al. 1996)

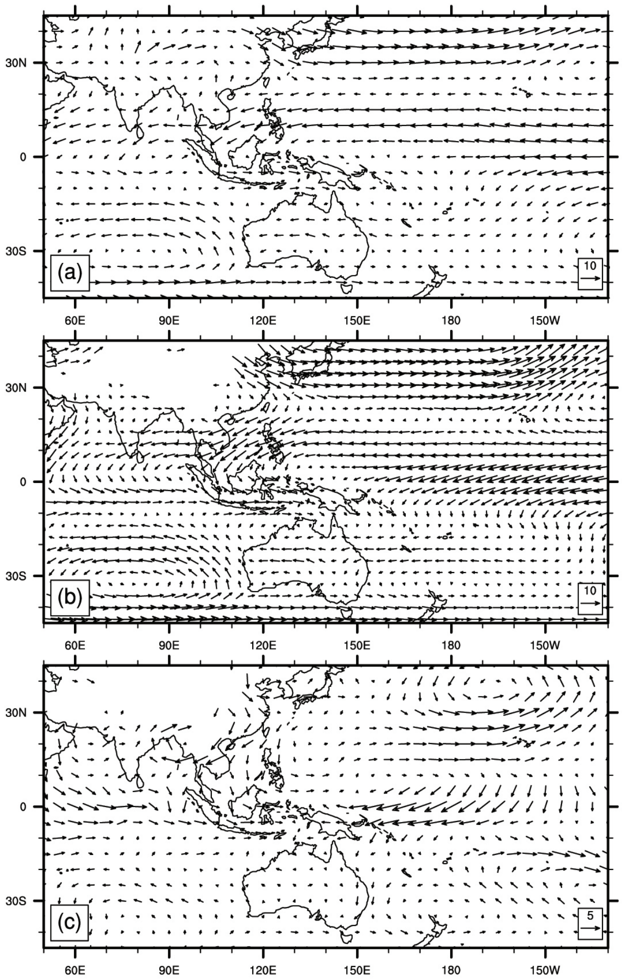

Fig. 6. Same as Fig. 5, but for the 200 hPa level.

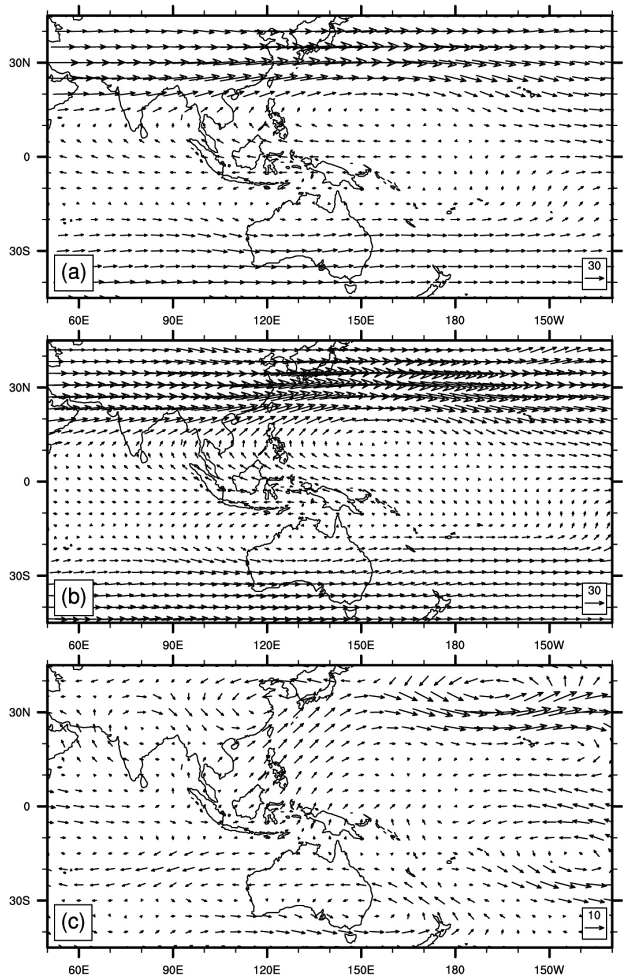

the tropics and are weaker at the upper level compared to the lower level (Fig. 5). The model captures the observed large-scale circulation features, although there are some discrepancies in the wind speed magnitudes particularly over the northern Pacific Ocean, east Asia and to some extent over eastern Australia.

Observed and modelled DJF rainfall is shown in Fig. 7. The pattern correlation between the observed and modelled spatial pattern is 0.8 and the RMS error is 2.3 mm/day. Analysis of CMIP3 datasets generated using the earlier CSIRO-Mk3.0 model showed a pattern correlation of 0.95 and an RMS error value of 1.0 mm/day (Suppiah et al. 2007). These statistics suggest that the CSIRO-Mk3.6 model shows stronger bias than the Mk3.0 version. An analysis of CMIP3 models by Colman et al. (2011) did show large range among the model skills and strong seasonality in spatial correlation over tropical Australian rainfall. CSIRO-Mk3.0 is no exception to other CMIP3 models. The current model (Mk3.6) does however reproduce the observed high rainfall regions over Indonesia and northern Australia and also the region east of Papua New Guinea. The low rainfall regions over the Asian continent, the subtropical regions of the northern Pacific Ocean and Australian continent are also represented accurately. The model tends to overestimate rainfall in the tropics between 60°E to 150°W and underestimates rainfall in the western equatorial Pacific Ocean.

The simulation of drier than observed conditions east of Papua New Guinea is likely the result of the cold tongue intrusion in the model, a phenomenon that is evident in most of the CMIP3 model simulations (Sun et al. 2006). Sun et al. (2006) emphasised that most of the models underestimate the strength of the negative feedback from cloud albedo and the strength of the negative feedback from atmospheric transport. The underestimate of the strength of these negative feedbacks is linked to an underestimate of the response of precipitation over the equator. Furthermore, all models have a stronger water vapor feedback than that indicated in Earth Radiation Budget Experiment (ERBE) observations (Sun et al. 2006). The zonal structure of rainfall over the southern hemisphere central and western Pacific Ocean indicates that the model partially captures the rainfall pattern associated with the South Pacific Convergence Zone

(SPCZ) (Brown et al. 2011). On the other hand, the model correctly simulates the southwest–northeast orientation of the rainfall zone over the Indian Ocean.

Links between DJF rainfall and atmospheric circulation

In this section, we evaluate how well the model simulates the relationship between rainfall and atmospheric circulation patterns on interannual timescales. Area-averaged DJF rainfall over the tropical Australian region (10–20ºS, 110–160ºE) for the period 1979–2005 was used to compute the correlation with the spatial distribution of mean sea level pressure, winds at 850 hPa (representing lower level) and 200 hPa (representing upper troposphere) levels in the wider region. The correlation shows the relationship between rainfall variability and atmospheric circulation patterns.

The observed and modelled relationships between mean sea level pressure and tropical Australian rainfall are shown in Fig. 8. The observed correlation (Fig. 8(a)) shows there is a strong negative correlation over most of Australia, with the minimum located over South Australia. In general, negative correlations cover a large area extending from the western Pacific Ocean, through southeast Asia and Australia, to the northern Indian Ocean. Positive correlations are found over the eastern Pacific Ocean and also the southern Indian Ocean, where the anti-cyclonic circulation dominates during summer.

The correlation pattern obtained using model results (Fig. 8(b)) shows strong negative correlations over the Maritime Continent, eastern Indian Ocean and most parts of Australia, with the minimum located over Australia's northwest. Although the model results show positive correlations over the eastern Pacific Ocean, unrealistic positive correlations are also found east of Papua New Guinea, presumably due to model bias resulting from the cold tongue. The broader picture suggests that the model pattern agrees reasonably well with the observed pattern, except over the Western Pacific warm pool. The Indonesian Archipelago, often referred to as the 'Maritime Continent' (Ramage 1968), is a significant area on the globe with respect to heat and moisture transfer between the ocean and the atmosphere. This region is often referred to as the Western Pacific Warm Pool, even though it extends into the eastern Indian Ocean.

The relationship between tropical Australian summer rainfall and low level tropospheric winds (850 hPa) is shown in Fig. 9. The correlations between the eastward/northward

Fig. 7. Observed (a) and simulated (b) climatologies for December–January–February rainfall for the period 1979–2005; and the difference between observed and simulated rainfall (c). Units are mm per day. Source for observational data: GPCP (Alder et al. 2003).

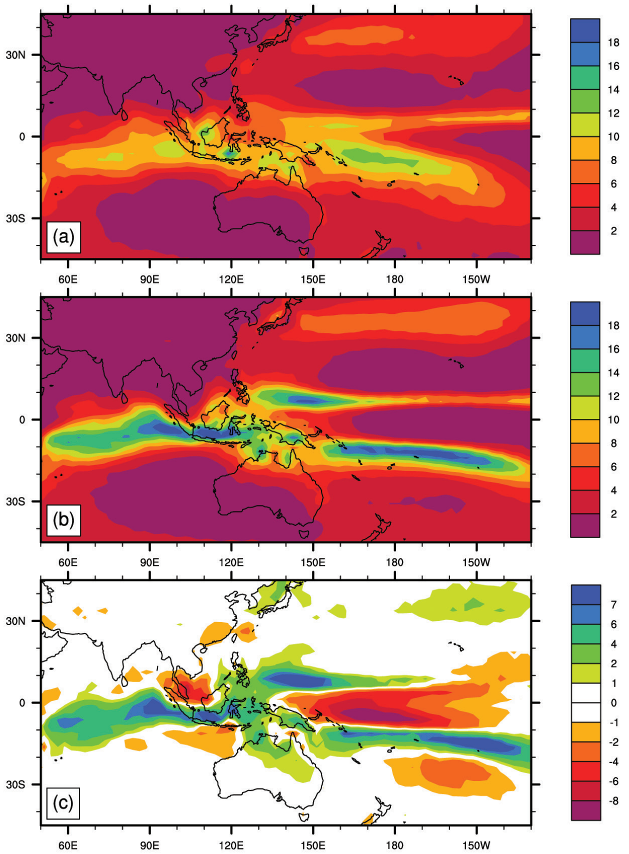

Fig. 8. Observed (a) and modelled (b) relationship between tropical Australian December–January–February rainfall and mean sea level pressure for the period 1971–2005. Stippling is used to show where the correlation is significant at the 95 per cent confidence level using a Student two-tailed *t*-distribution. Source for observation: Kalnay et al. (1996) and AWAP.

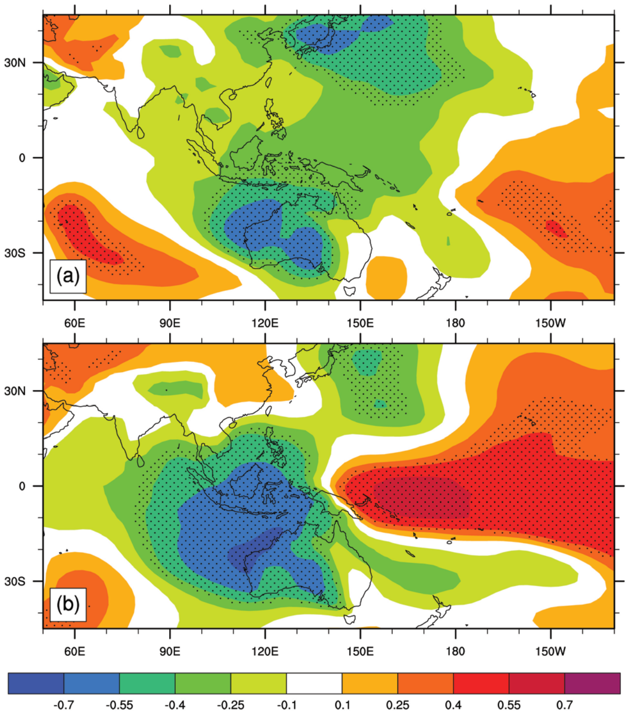

components and rainfall are shown as vectors. The observed pattern (Fig. 9(a)) indicates that tropical Australian summer rainfall is strongly linked to: (a) the cyclonic circulation over the northwestern part of Australia; (b) northeasterlies over southeast Asia; (c) southerlies off the southwestern coast of Australia; and (d) northeasterlies over eastern Australia. The pattern also indicates that an anti-cyclonic circulation over east Asia initiates southerlies that are known to have a significant impact on rainfall over tropical Australia (Suppiah and Wu 1998, Zhang and Zhang 2010). A comparison between the observed and modelled correlation patterns in Figs 9(a) and 9(b) suggests that the model captures the link between the major circulation regimes and tropical Australian rainfall variability. In particular, the links with the major cyclonic circulation over northwestern Australia, westerlies over Indonesia and northern Australia, and northerlies from east Asia are captured. However, the model simulates a cyclonic-type circulation over the South China Sea which is not found in the observations.

Due to the intrusion of the cold tongue over the western Pacific Ocean, the model generates some circulation features which are not realistic. The confluence of strong easterlies over the western Pacific Ocean north of Papua New Guinea, strong westerlies over the Indonesian region, and northeasterlies over southeast Asia, form a cyclonic-type circulation east of the Philippines. The major cyclonic system over northwestern Australia is also shifted westward, and hence, weak southerlies prevail over the southern central Indian Ocean. These discrepancies are mainly due to unusually strong easterlies over the western Pacific Ocean.

The relationship between tropical Australian summer rainfall and upper level tropospheric winds (200 hPa) is shown in Fig. 10. The model captures the link between rainfall and the anti-cyclonic circulations over the Australian continent and east Asia. The model however fails to capture the relationship over the equatorial Pacific Ocean. It is also worth mentioning that the relationship between tropical Australian rainfall variability and upper level circulation simulated by the model is not as strong as the relationship between rainfall variability and low level circulation (Fig. 9).

Figure 11 shows the observed climatological sea surface temperatures (SSTs) over the Indian and western Pacific Oceans, and the biases between model simulations and observations. It is evident that relatively cooler temperatures are simulated east of Papua New Guinea, coastal regions of southeast Asia, parts of the northern Pacific Ocean, and a region over the eastern Indian Ocean centred around 20°S, west of Western Australia. The strong bias in the Indian Ocean and northern Arabian Sea will likely have a significant impact on the simulation of the Indian Ocean Dipole. The observed SSTs are however well captured by the model in the equatorial region (10°S–10°N) west of Papua New Guinea.

The spatial patterns of the relationship between the NINO3.4 index and observed and simulated rainfall is shown in Figs 12(a) and (b), respectively. The observed relationship (Fig. 12(a)) indicates below normal rainfall over the western

Fig. 9. Observed (a) and modelled (b) relationships between tropical Australian December–January–February rainfall and winds at the 850 hPa level for the period 1971–2005. Correlations are shown using a vector scale between 0–1. Pink shading is used to show areas where the wind speeds (not shown) are statistically significant at the 95 per cent confidence level using a Student two-tailed t-distribution. Source of observation: Kalnay et al. (1996) and AWAP.

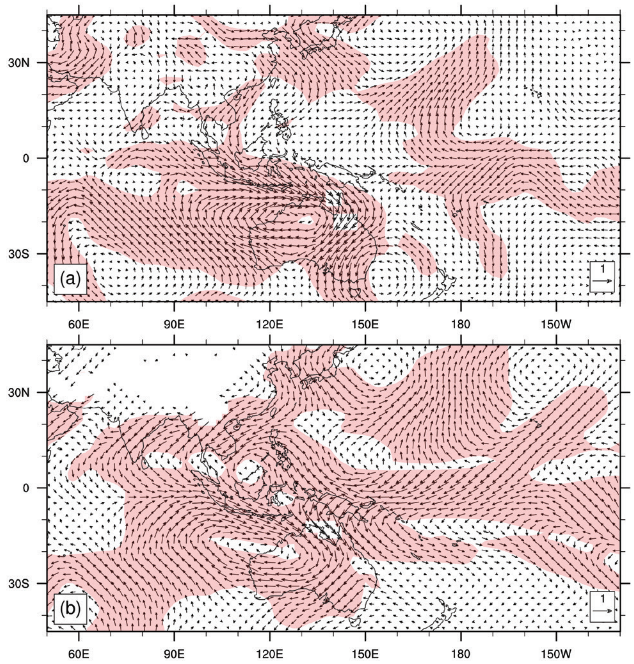

Fig. 10. Same as Fig. 9, but for the 200 hPa level.

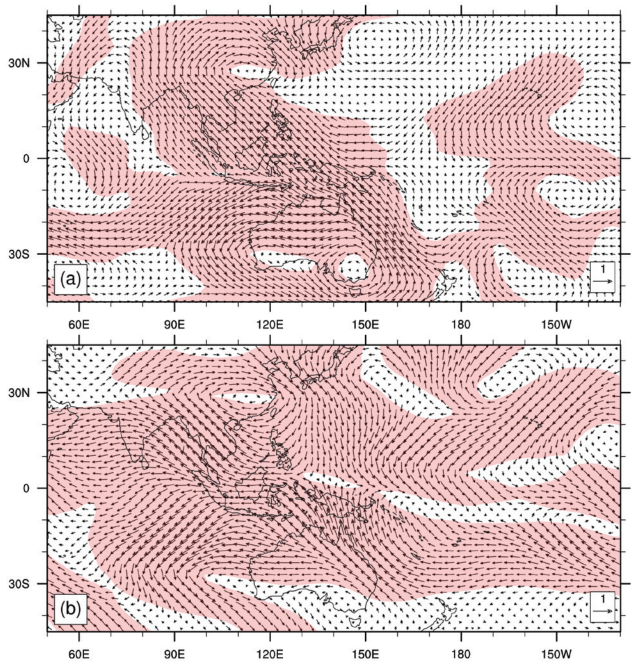

Fig. 11. Observed (a) December–January–February climatological SSTs during the Australian monsoon season, and the differences between CSIRO-Mk3.6 simulated December–January–February SSTs and observed SSTs (b). In the upper panel, SSTs are shown by actual values and in the lower panel as anomalies in degrees Celsius. Source for observations: HadISST (Rayner et al. 2006).

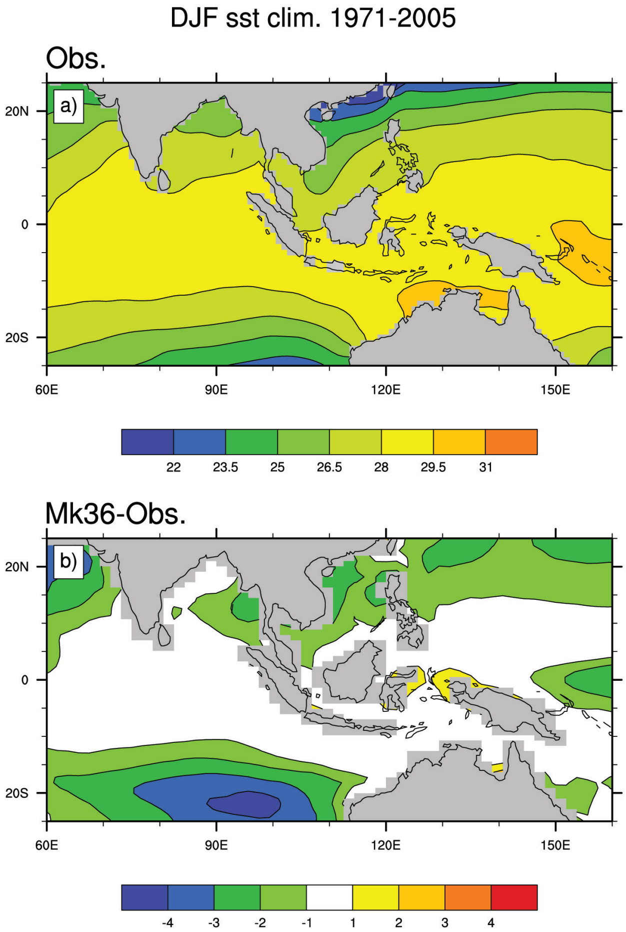

Pacific and eastern Indian Oceans, with a strong relationship over a region east of the Philippines. Above normal rainfall is observed over the central to south Indian Ocean region centred around 30°S, and also in the tropics centred around 160°E. Compared to the observed spatial relationship, the model weakly captures the spatial pattern of the link between the El Niño-Southern Oscillation phenomenon and summer monsoon rainfall over tropical Australia and the western Pacific Ocean. The model simulates relatively stronger rainfall anomalies north of Papua New Guinea, which extend further westward compared to observations. Such westward extension of rainfall anomalies can be attributed to the cold tongue intrusion in the simulation.

In the remainder of this section, we investigate whether the existing relationships between tropical Australian rainfall variability and atmospheric circulation are expected to continue under anthropogenic climate change conditions. In Fig. 13 we show the simulated correlation between rainfall and mean sea level pressure (a); and winds at lower

Fig. 12. Regression coefficients showing the relationships between observed (a) and modelled (b) December–January–February rainfall and the December–January–February NINO3.4 index. Units are mm/day per K. Source for observations: HadISST (Rayner et al. 2006).

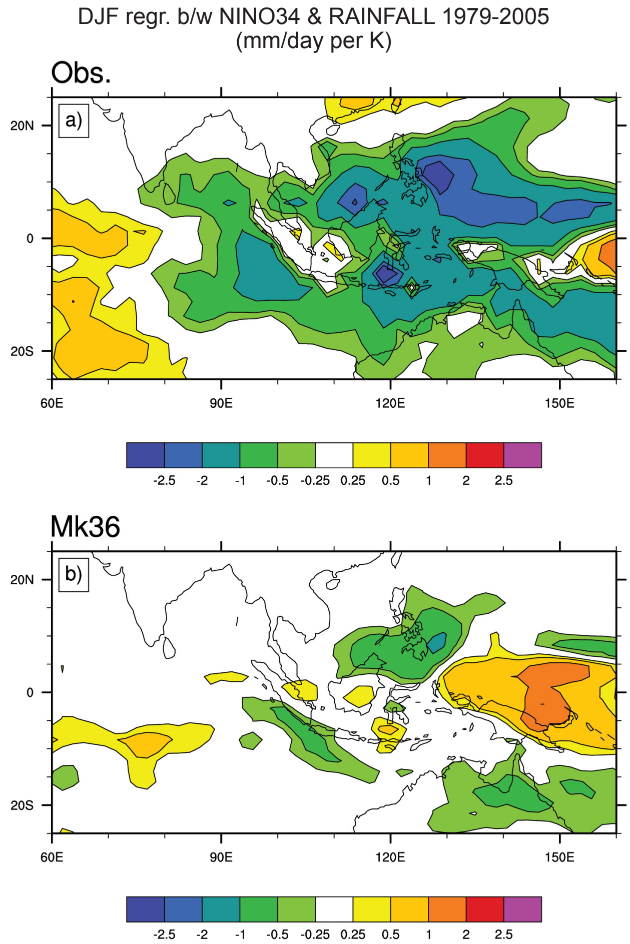

and upper levels (b and c, respectively) for the period 2066–2100. Comparison of the correlation maps for the historical (Fig. 8(b)) and projection (Fig. 13(a)) periods shows that the model maintains the relationship between tropical Australian rainfall and mean sea level pressure (over the selected domain) under anthropogenic climate change condition. In both periods a negative relationship over the northwestern Australia and positive relationship over east of Papua New Guinea are simulated. Comparison of the two figures shows the projected relationship is relatively weaker than the historical relationship, particularly over the western and central parts of Australia and the region east of Papua New Guinea.

The spatial relationship between tropical Australian rainfall and winds at the 850 hPa level is shown in Fig. 13(b). Comparison of the projected relationship with the historical relationship in Fig. 9(b) suggests that the model maintains the relationship under climate change conditions, albeit strengthened over the region north of Australia and weakened over the Australian continent. The changes are accompanied by an increase in the relationship with

Fig. 13. Projected correlations between tropical Australian December–January–February rainfall and mean sea level pressure (a), winds at the 850 hPa (b) and winds at the 200 hPa (c) for the period 2066–2100 using the RCP 8.5 emissions scenario. In the top panel, stippling is used to show where the correlations are significant at the 95 per cent confidence level using a Student two-tailed t-distribution. In the middle and lower panels the correlations are shown using a vector scale, with pink shading used to show areas where the wind speeds (not shown) are statistically significant at the 95 per cent confidence level using a Student two-tailed t-distribution. Units of correlations are shown between 0 and 1.0 in vector scale.

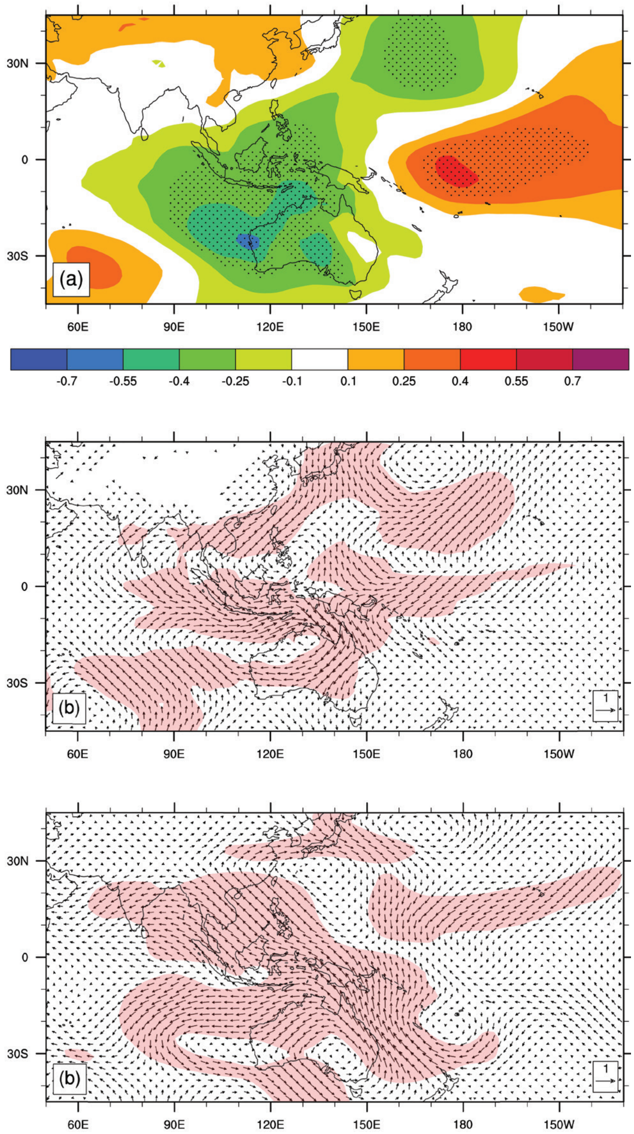

westerlies over Indonesia. A cyclonic type circulation (shown by vectors) over the Philippines is also strengthened, but this feature is not evident in the observed historical pattern (compare Figs 9(a) and 9(b)).

The spatial pattern of the relationship between tropical Australian rainfall and winds at the 200 hPa level is shown in Fig. 13(c). The projected relationships are very similar to the simulated historical relationships in Fig. 10(b). However, the relationship over the northern hemisphere suggests some changes are expected to occur, with the anti-cyclonic region projected to move eastward over east Asia.

Projected changes in mean sea level pressure, winds and rainfall

In this section we investigate the projected changes in mean sea level pressure, winds and rainfall under RCPs 4.5 and 8.5. The simulated patterns of change in mean sea level pressure, winds and rainfall are very similar under both scenarios, but the signal is stronger under RCP8.5. We therefore discuss results for both scenarios, but only present figures for RCP 8.5. The projected changes in mean sea level pressure, lower and upper (850 and 200 hPa) winds and rainfall under the RCP 8.5 emissions scenario are shown in Figs 14(a, b, c, d), respectively. The changes are shown as the differences between the mean values for the two periods 2066–2100 and 1979–2005. Fig. 14(a) shows strong increases in mean sea level pressure are expected over a broad region centred off northwest Australia and over the northern Pacific Ocean. In contrast, a stronger decrease is expected in the central Asia region. Although the pattern for RCP 4.5 is similar the changes in mean sea level pressure magnitudes are smaller. The projected increase in mean sea level pressure over northwest Australia and decrease over central Asia implies a weakening of the pressure gradient during summer, and therefore a possible weakening of the Australian monsoon. Comparison with other studies on the Australian monsoon (for example, Colman et al. 2011) is not yet possible, as most existing work has not used a sufficiently large domain to identify the link between central Asia and the Australian continent.

The projected changes in lower and upper level winds (Figs 14(b) and (c), respectively) also imply a weakening of the monsoon. The weakening is suggested by expected changes in easterlies at the lower tropospheric level (850 hPa) and westerlies at the upper tropospheric level (200 hPa). Consistent with projected changes in atmospheric circulation under anthropogenic climate change conditions, the model simulates a decrease in rainfall (Fig. 14(d)) over Indonesia, northern Australian and around the Philippines. However, the model also simulates an increase in rainfall east of Papua New Guinea and also over Indian Ocean, south of the Indian continent. The model simulates a decrease in tropical Australian rainfall of about twenty per cent under RCP 4.5 and about 30 per cent under RCP 8.5. While the spatial patterns of change under both RCPs 4.5 and 8.5 are very similar, the magnitudes of the expected changes are enhanced under RCP 8.5. Comparison of the current projections from CSIRO-Mk3.6 with those from earlier versions of the model (CSIRO-Mk3.0 and CSIRO-Mk3.5) shows the Mk3.6 projections are comparable with the earlier results. CSIRO-Mk3.0 simulated about a two per cent increase, while CSIRO-Mk3.5 GCM simulated about a

Fig. 14. Projected December–January–February changes in: (a) mean sea level pressure in hPa; (b) wind at the 850 hPa level in m/s; (c) wind at the 200 hPa level in m/s; (d) rainfall in mm/day; and (e) SST in K under RCP 8.5. Changes are calculated as the differences between the period 2066–2100 and the historical period 1971–2005.

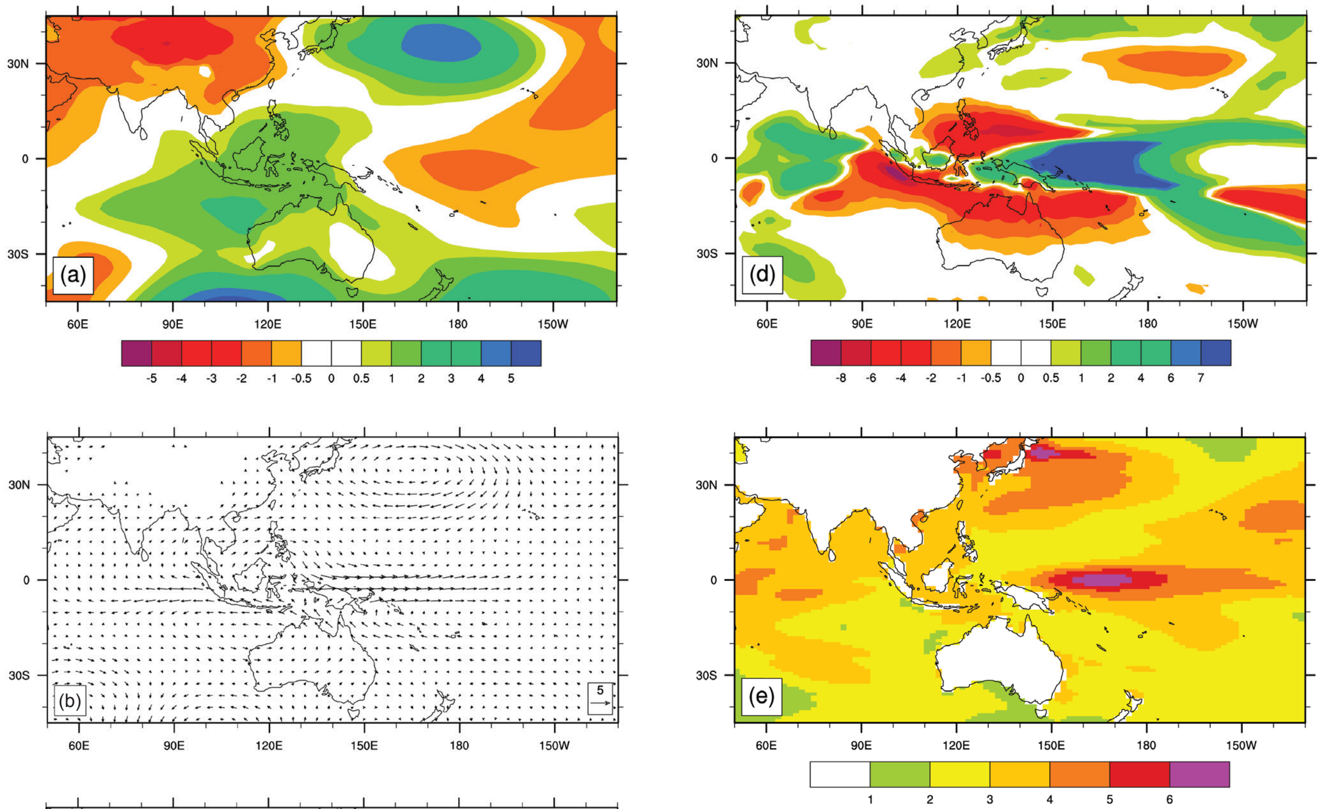

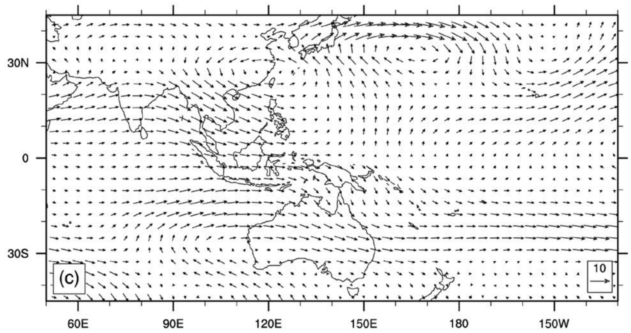

six per cent decrease in summer rainfall (Suppiah et al. 2013). Compared to the previous versions of the model, the Mk3.6 model simulates a greater decrease over tropical Australia.

In another study, Watterson (2012) established a strong negative relationship between projected rainfall changes over the Australian continent (including the tropics) and the projected difference in SSTs over the western Pacific and eastern Indian oceans using CMIP3 simulations. The index derived from SST anomalies, the so-called Pacific Indian Ocean Dipole (PID), is relatively large for CSIRO-Mk3.0 and Mk3.5, and is consistent with the relatively strong projected tropical rainfall declines in these models compared to most other CMIP3 models. Similar to previous versions of the model, Mk3.6 also shows greater warming over east of Papua New Guniea and less warming over eastern Indian Ocean (Fig. 14(e)). This pattern of warming leads to decreased rainfall over tropical Australia.

Figure 15 shows projected changes in selected precipitation extremes indices, as defined by the Australian Bureau of Meteorology[1]. The indices were computed for the summer season in tropical Australia around 2085 under the RCP 8.5 emissions scenario. The indices are as follows: (a) very wet day precipitation (annual total precipitation from all days with precipitation >95th percentile value); (b) extremely wet day precipitation (annual total precipitation from all days with precipitation >99th percentile value); (c) heavy precipitation days (annual count of days with daily precipitation ≥10 mm); and (d) very heavy precipitation days (annual count of days with daily precipitation ≥30 mm). The projections show that tropical Australia may experience a decline in the number of heavy and very heavy precipitation days as well as a decrease in very wet day precipitation. However, the projections show an increase in extremely wet day precipitation in northernmost Australia during the 21st century.

[1]http://www.bom.gov.au/climate/change/about/extremes.shtml

Fig. 15. Projected December–January–February changes under RCP 8.5 around 2085 in: (a) very wet day rainfall; (b) extremely wet day rainfall; (c) heavy rainfall days; and (d) very heavy rainfall days. Stippling areas indicate statistical significance at the 95 per cent confidence level.

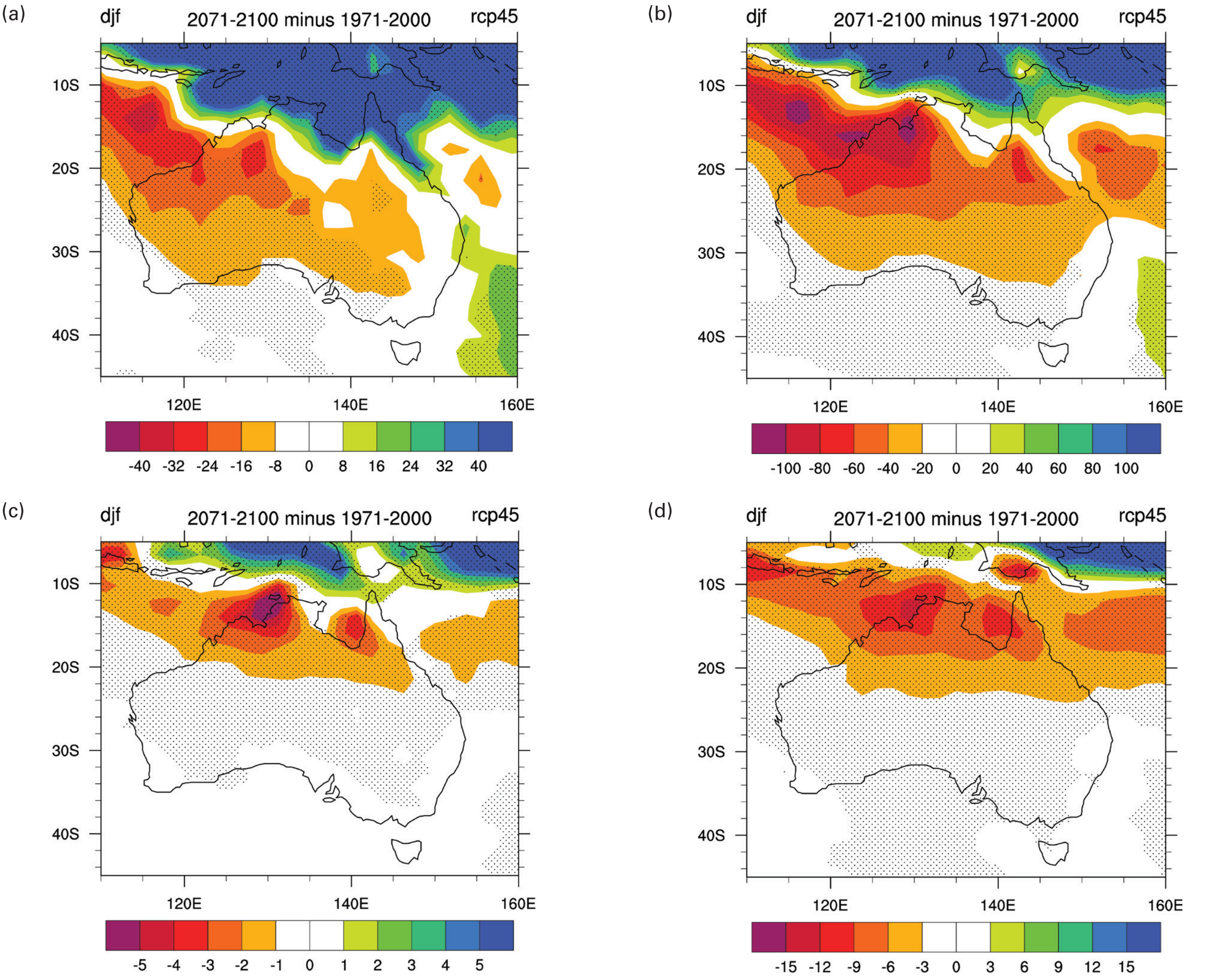

Conclusion

In this study we assessed the results from an ensemble of CMIP5 simulations with the CSIRO-Mk3.6 climate model. The results of historical simulations for mean DJF rainfall, mean sea level pressure and both low and high-level tropospheric winds have been compared to observations, as well as the links between rainfall and various atmospheric variables. The comparisons show that the model captures the spatial structures of the observed patterns but there are some discrepancies between the magnitudes of the observed and modelled parameters. The model also captures the observed link between tropical Australian rainfall variability and atmospheric circulation patterns in summer. The link between rainfall variability and low level circulation was found to be stronger than the link with upper tropospheric level circulation.

The model weakly captures the observed spatial relationship of the link between the El Niño-Southern Oscillation phenomenon and summer monsoon rainfall over tropical Australia. In the historical experiment, the model simulates relatively stronger rainfall anomalies region north of Papua New Guinea, which extend further westward compared to observations.

Under anthropogenic climate change conditions, the CSIRO-Mk3.6 model predicts a weakening of the Australian monsoon and reduced rainfall over tropical Australia. The projected weakening of the monsoon circulation and reduction in rainfall are both stronger under RCP 8.5 than RCP 4.5, although the simulated spatial patterns are very similar under both scenarios. An increase in pressure over northwest Australia and a slight decrease in pressure over northern Asia are simulated, which in turn produce a weaker pressure gradient under climate change conditions. Projections for winds at lower and upper levels indicate opposing trends, while rainfall is expected to decline over a broad region that encompasses northern Australia, parts of Indonesia and the Philippines. The cyclonic circulation pattern over northwestern Australia is displaced westward as a result of cold tongue intrusion simulated by the model. However, an increase in rainfall is simulated for the region east of Papua New Guinea. Similar to mean rainfall change, the model simulates a decrease in heavy rainfall events under anthropogenic climate change conditions. Compared to the previous version of the model (CSIRO-Mk3.0 and Mk3.5), the CSIRO-Mk3.6 model simulates a greater decrease in rainfall over tropical Australia by the end of the century. It is also worth mentioning that differences in projected changes in atmospheric circulation and rainfall between CSIRO-Mk3.0, Mk3.5 and Mk3.6 are not just developments and changes to model, but also could be due to different emission scenarios, i.e. SRES versus RCPs.

Acknowledgments

Martin Dix from CSIRO provided Fig. 1. Ian Smith assisted with editing which significantly improved the paper. The study has been funded by the ACCSP Australian Monsoon Project.

References

Adler, R.A., Huffman, G.J., Chang, A., Ferraro, R., Xie, P-P., Janowiak, J., Rudolf, B., Schneider, U., Curtis, S., Bolvin, D., Gruber, A., Susskind, J., Arkin, P. and Nelkin, E. 2003. The Version-2 Global Precipitation Climatology Project (GPCP) Monthly Precipitation Analysis (1979–Present). *J. Hydrometer., 4,* 1147–67.

Brown, J.R., Power, S.B., Delage, F.P., Colman, R.A., Moise, A.F. and Murphy, B.F. 2011. Evaluation of the South Pacific Convergence Zone in IPCC AR4 Climate Model Simulations of the Twentieth Century. *J. Clim., 24,* 1565–82.

Collier, M.A., Jeffrey, S.J. and Rotstayn, L.D. 2011a. The latest Australian CMIP climate model submission. *Bull. Aust. Met. Oceanogr. Soc., 24,* 103–8. http://www.amos.org.au/documents/item/589.

Collier, M.A., Jeffrey, S.J., Rotstayn, L.D.,Wong, K.K-H., Dravitzki, S.M., Moeseneder, C., Hamalainen, C., Syktus, J.I., Suppiah, R., Antony, J., El Zein, A. and Atif, M. 2011b. The CSIRO-Mk3.6.0 Atmosphere-Ocean GCM: participation in CMIP5 and data publication. *19th International Congress on Modelling and Simulation*, Perth, Australia, 12–16 Dec., 1–7.

Colman, R., Moise, A.F. And Hanson, L.I. 2011. Tropical Australian climate and the Australian monsoon as simulated by 23 CMIP3 models. *J. Geophys. Res., 116*. D10116, doi.10.1029/2010JD015149,2011.

CSIRO and Bureau of Meteorology 2007. *Climate change in Australia*. CSIRO Technical Report http://www.climatechangeinaustralia.com.au/resources.php.

Gordon, H.B., Rotstayn, L.D., McGregor, J.L., Dix, M.R., Kowalczyk, E.A., O'Farrell, S.P., Waterman, L.J., Hirst, A.C., Wilson, S.G., Collier, M.A., Watterson, I.G. and Elliott, T.I. 2002. *The CSIRO Mk3 Climate System Model*, CSIRO Atmospheric Research Technical Paper No. 60., 134 pp. Available online at http://www.cmar.csiro.au/e-print/open/gordon_2002a.pdf.

Gordon, H.B., O'Farrell, S.P., Collier, M.A., Dix, M.R., Rotstayn, L.D., Kowalczyk, E.A., Hirst, A.C. and Watterson, I.G. 2011. *The CSIRO Mk3.5 Climate Model*. Technical Report No. 21, The Centre for Australian Weather and Climate Research, Aspendale, Vic., Australia, 62 pp., available at: http://www.cawcr.gov.au/publications/technicalreports.php.

IPCC, 2007. *Climate Change 2007: The Physical Science – Summary for Policymakers*. Contribution of Working Group I to the Fourth Assessment Report of the Intergovernmental Panel on Climate Change, 17pp.

Jeffrey, S.J., Rotstayn, L.D., Collier, M.A., Dravitzki, S.M., Hamalainen, C., Moeseneder, C., Wong, K.K. and Syktus, J.I. 2013. Australia's CMIP5 submission using the CSIRO Mk3.6.0 model. *Aust. Meteorol. Oceanogr. J.*, 63, 1–13.

Jones, D.A., Wang, W. and Fawcett, R. 2009. High-quality spatial climate data-sets for Australia, *Aust. Met. Oceanogr. J., 58,* 233–48.

Klingaman, N., Woolnough, S. and Syktus, J. 2012. On the drivers of inter-annual and decadal rainfall variability in Queensland, Australia. *Int. J. Climatol.*, ISSN 0899-8418 doi: 10.1002/joc.3593

Kalnay, E., Kanamitsu, M., Kistler, R., Collins, W., Deaven, D., Gandin, L., Iredell, M., Saha, S.,White, G., Woollen, J., Zhu, Y., Chelliah, M., Ebisuzaki, W., Higgins, W., Janowiak, J., Mo, K. C., Ropelewski, C., Wang, J., Leetmaa, A., Reynolds, R., Jenne, R. and Joseph, D. 1996. The NCEP/NCAR40-year reanalysis project. *Bull. Am. Meteorol. Soc., 77,* 437–71.

Kim, H-J., Wang, B. and Ding, Q. 2008. The global monsoon variability simulated by CMIP3 coupled climate models. *J. Clim., 21,* 5271–93.

Meinshausen, M., Smith, S.J., Calvin, K., Daniel, J.S., Kainuma, M.L.T., Lamarque, J-F., Matsumoto, K., Montzka, S.A., Raper, S.C., Riahi, K., Thomson, A., Velders, G.J.M. and Vuuren, van D.P.P. 2011. The RCP greenhouse gas concentrations and their extensions from 1765 to 2300. *Climatic Change, 109,* 213–41.

Räisänen, J. 2007. How reliable are climate models? *Tellus, 59A,* 2–29.

Ramage, C.S. 1968. Role of a tropical 'maritime continent' in the atmospheric circulation. *Mon. Weather Rev. 96,* 365–70.

Rayner, N.A., Parker, D.E., Horton, E.B., Folland, C.K., Alexander, L.V., Rowell, D. P., Kent, E.C. and Kaplan, A. 2006. Global analyses of sea surface temperature, sea ice, and night marine air temperature since the late nineteenth century. *J. Geophys. Res., 108,* No. D14, 4407 10.1029/2002JD002670.

Risbey, J.S. Pook, M.J., McIntosh, P.C., Wheeler, M.C. and Hendon, H.H. 2009. On the remote drivers of rainfall variability in Australia. *Mon. Weather Rev., 137,* 3233–53.

Rotstayn, L.D., Jeffrey, S.J., Collier, M.A., Dravitzki, S.M., Hirst, A.C., Syktus, J.I. and Wong, K.K. 2012. Aerosol- and greenhouse gas-induced changes in summer rainfall and circulation in the Australasian region: a study using single-forcing climate simulations. *Atmos. Chem. Phys., 12,* 6377–404, doi:10.5194/acp-12-6377-2012.

Smith, I.N. 2007. Climate modelling within CSIRO: 1981 to 2006. *Aust. Meteorol. Mag., 56,* 131–52.

Smith, I.N. and Chandler, E. 2009. Refining rainfall projections for the Murray Darling Basin of south-east Australia – the effect of sampling model results based on performance. *Climatic Change, 102,* 377–93.

Smith, I.N., Moise A.F. and Colman, R.A. 2012. Large scale circulation features in the tropical western Pacific and their representation in climate models. *J. Geophy. Res., 117,* D04109, doi:10.1029/2011JD016667.

Sun, D.-Z., Zhang, T., Covey, C., Klein, S. A., Collins, W.D., Hack, J.J., Kiehl, J.T., Meehl, G.A., Held, I.M. and Suarez M. 2006. Radiative and dynamical feedbacks over the equatorial cold-tongue: Results from nine atmospheric GCMs. *J. Clim., 19,* 4059–74.

Suppiah, R. and Wu, X. 1998. Surges, cross-equatorial flows and their links with the Australian summer monsoon circulation and rainfall. *Aust. Meteorol. Mag., 47,* 113–30.

Suppiah, R., Hennessy, K.J., Whetton, P.H., McInnes, K., Macadam, I., Bathols, J., Ricketts, J. and Page, C.M. 2007. Australian climate change projections derived from simulations performed for the IPCC 4th assessment report. *Aust. Meteorol. Mag., 56,* 131–52.

Suppiah, R., Watterson, I.G., Macadam, I., Collier, M. and Bathols, J. 2010. *Climate change projections for the tropical rainforest region of north Queensland*. Final report on MTSRF Research, 2006–2010. Reef and Rainforest Research Centre, Cairns, 69p.

Suppiah, R., Moise, A., Colman, R. and Hanson, L. 2012. Circulation of anomalous wet and dry Australian monsoon seasons and future changes from CMIP3 simulations. Abstracts, CAWCR Monsoon Workshop, 15 November 2012.

Taylor, K.E., Stouffer, R.J. and Meehl, G.A. 2012. An overview of CMIP5 and the experiment design. *Bull. Am. Meteorol. Soc.*, April 2012, 485–98.

Watterson, I.G. 2012.Understanding and partitioning future climates for Australian regions from CMIP3 using ocean warming indices. *Climatic Change, 111,* 903–22.

Williams, S.E., Shoo, L., VanDerWal, J. and Williams. Y. 2010. Understanding and protecting rainforest biodiversity: adapting to global climate change. Presentation to the *2010 Annual Conference of the Marine and Tropical Sciences Research Facility (MTSRF),* 18–20 May 2010, Cairns.

Zhang, C. and Zhang, H. 2010. Potential impacts of East Asian winter monsoon on climate variability and predictability in the Australian summer monsoon region. *Theor. Appl. Climatol., 101,* 161–77.